# Regular anisotropic filtering and multi-level thresholding for image segmentation

**Slim BEN CHAABANE**[1,2]

[1]Computer and Information Technology Faculty, Tabuk University.
Kingdom of Saudi Arabia - PO Box: 4279 - Tabuk: 71491

[2] SIME Research Laboratory, ENSIT University of Tunis,
5 Av. Taha Hussein, 1008, Tunis, Tunisia

*s.chaabane@ut.edu.sa*

Abstract: ***In this article, we present a new image segmentation method, based on anisotropic filtering and multilevel thresholding. For segmentation, we proceed in two steps. In the first step, anisotropic filtering technique is used to filter the original image. In the second step, we identify the most significant peaks of the histogram. For this purpose, an optimal multi-level thresholding is used based on the two-stage Otsu optimization approach. The algorithm is demonstrated through the segmentation of textured images .***
***The classification accuracy of the proposed method is evaluated and a comparative study versus existing techniques is presented. The experiments were conducted on an extensive set of gray level images. Satisfactory segmentation results have been obtained showing the effectiveness and superiority of the proposed method.***
**Keywords:** Segmentation, multilevel thresholding, denoising image, anisotropic Diffusion, the two stage multithreshold Otsu method.

## 1. Introduction

Image denoising and segmentation are fundamental problems in the field of image processing and computer vision. Image denoising is a technique that enhances images by reducing any degradations that may be present. Image segmentation is the first step in image analysis and pattern recognition. It is one of the most difficult tasks in image processing, which determines the quality of the final segmentation [1]. It can be considered as a pixel labeling process in the sense that all pixels that belong to the same homogeneous region are assigned with the same label. However, the major problem in image segmentation is the presence of noise.
Several approaches of different complexity already exist to gray level image segmentation [2] [3]. Until now, there is no general technique that can solve all the different image types. In this context, several algorithms have been proposed in literatures that have addressed the issue of histogram thresholding [4] [5] [6]. The most widely used clustering method is the Otsu's method [6]. The major problem of this method resides in the determination of the optimal thresholds, especially if there is a large class number required in the image. However, several methods have been proposed to greatly improve the efficiency of Otsu's method. Recently, D. Y. Huang et al. [7] have presented a new fast algorithm called the two stage multithreshold Otsu method. This algorithm is used to reduce the large number of iterations required by Otsu's method for computing the cumulative probability and the mean of a class.
Denoising image is an important research area in image processing. It is a very important pretreatment to image for the further research and process. The general denoising problem involves removing the noise and recovering the true image. Alternatively, denoising image can be achieved by averaging. Many techniques have been proposed in the literature dealing the denoising image problem [8]. In fact, the denoising image problems have been reported in diverse publications [8]. For instance, several authors applied different techniques for improving image-denoising results.
Traditional techniques such as box filtering and Gaussian filtering treat all pixels equally during the denoising process, which leads to the unwanted blurring of perceptually significant characteristics.
However, several techniques in the spatial domain denoising have been proposed that used to suppress noise while preserving such image characteristics. These newer denoising techniques include anisotropic filtering [8], total variation [9], bilateral filtering [10] [11], and non-local means filtering techniques [12] [13]. In the same context of denoising image, the transform domain denoising techniques are those that first convert an image into a transform domain and then alters the transform coefficients to reduce noise. Some transform domain techniques include Wiener filtering [14] and wavelet based techniques [15] [16].
In this paper, a new segmentation method is presented. For segmentation, we proceed in two steps. In the first step, the anisotropic diffusion technique is employed to suppress noise while preserving the important information's. In the second step, we identify the most significant peaks of the histogram. For this purpose, an optimal multi-level thresholding is used based on the two-stage Otsu optimization approach.
The paper is organized as follows. Section 1 introduces the proposed segmentation method. The experimental results are discussed in section 3, and the conclusion is given in section 4.

## 2. Introduction

In the framework of our application, we are interested in gray level image segmentation of textured images. The problem is to segment the input images into homogeneous regions. The

first step of the proposed method is to remove the noise and recovering the true image. In the second step, the TSMO [7], is applied on the filtered image.

### 2.1. Modified Anisotropic filtering

The anisotropic diffusion was introduced by Perona and Malik [17]. It is a class of filter that reduces noise in an image while trying to preserve sharp edges. This algorithm anisotropically diffuses an image, i.e., objects are blurred, but their edges are blurred by a lesser amount. Hence, this algorithm blurs over homogeneous regions but diffuses little over nonhomogeneous regions.
Assume $I(x,y)$ is the intensity of a pixel $p(x,y)$ at the location $(x,y)$ in an image I, which defined as a limited application of $\Omega \subset R2 \to R$. $\Omega$ is the field of the image. Let use denote $I_0(x,y) = I_0$ the noisy image.
The anisotropic diffusion is represented by:

$$\begin{cases} \dfrac{\partial I(x,y,t)}{\partial t} = div(c\|\nabla I(x,y,t)\|)\nabla I(x,y,t) \\ I(x,y,0) = I_0(x,y) \\ \dfrac{\partial I}{\partial \Omega}\Big|_{\partial\Omega} = 0 \end{cases}$$

where $c(.)$ called diffusion function, is a nonnegative, monotonous decreasing function, such as $c(0) = 1$. Typically, a function of the gradient magnitude $\|\nabla I\|$.
The differences with the closest neighbors in the four directions (North, South, Est, ouest) and the diffusion coefficient are calculated as follow:

$$\nabla_N I_{i,j} = I_{i-1,j} - I_{i,j}, c_{N_{i,j}} = g\left(\left|\nabla_N I_{i,j}\right|\right)$$
$$\nabla_S I_{i,j} = I_{i+1,j} - I_{i,j}, c_{S_{i,j}} = g\left(\left|\nabla_S I_{i,j}\right|\right)$$
$$\nabla_E I_{i,j} = l_{i,j+1} - l_{i,j}, c_{E_{i,j}} = g\left(\left|\nabla_E I_{i,j}\right|\right)$$
$$\nabla_w I_{i,j} = I_{i,j-1} - I_{i,j}, c_{w_{i,j}} = g\left(\left|\nabla_w I_{i,j}\right|\right)$$

where the function $g$ is defined as:

$$g(|\nabla I|) = e\left(-\left(\left\|\frac{\nabla_I}{k}\right\|\right)^2\right)$$

k is a threshold, used to distinguish the zones with weak gradient from those with strong gradient. In our application, k is fixed to 0.1.

### 2.2. Recursive Otsu Method for Multilevel thresholding

The Histogram thresholding is used in our application to segment the gray level image into homogeneous regions. To do this, we use an algorithm called the Two-stage Multithreshold Otsu's method (TSMO). A general concept of the TSMO method is given in Ref. [7].
The idea of this method is to gray level image into M class. In the first stage of the TSMO method, the histogram of an image with **L** gray levels is divided into $M_z$ groups, which contain $N_z$ gray levels.
In this study, the groups of the total image space **Ω** composed of $M_z$ groups, are symbolized by:

$$\Omega = \{\Omega_j | j = 0, 1, 2, \dots, M_{z-1}\}$$

where $j$ represents the group number.
Precisely, each group contains a certain range of gray levels as follows:

$$\begin{cases} \Omega_0 = \{0, 1, 2, \dots, N_z - 1\} \\ \Omega_1 = \{N_z, N_z + 1, \dots, 2\mathrm{N_z} - 1\} \\ \qquad\qquad \dots \\ \qquad\qquad \dots \\ \Omega_q = \{qN_z, qN_z + 1, \dots, (\mathrm{q}+1)\mathrm{N_z} - 1\} \\ \Omega_{\mathrm{M_z}-1} = \{(\mathrm{M_z}-1)N_z, (\mathrm{M_z}-1)N_z + 1, \dots, \mathrm{M_z N_z} - 1\} \end{cases}$$

The number of cumulative pixels, in the $q^{th}$ group denoted by $g_{\Omega_q}$ can be calculated as:

$$g_{\Omega_q} = \sum_{i=q\times N_z}^{(q+1)\times N_z - 1} f_i$$

where $f_i$ represents the number of pixels with gray level $i$. Since each group contains gray levels, the corresponding gray level value for each group can be considered as a mean value for those gray levels. Therefore, the corresponding gray level value or mean intensity, in the $q^{th}$ group denoted by $i_{\Omega_q}$ can be calculated as:

$$i_{\Omega_q} = \frac{\sum_{i=q\times N_z}^{(q+1)\times N_z - 1} i f_i}{\sum_{i=q\times N_z}^{(q+1)\times N_z - 1} f_i} = \frac{1}{g_{\Omega_q}} \sum_{i=q\times N_z}^{(q+1)\times N_z - 1} i f_i$$

Hence, The TSOM can be applied to find the optimal threshold $j^*$ by maximizing the between-class variance $(\sigma_B^2)$ with the sets of $i_\Omega$ and $g_\Omega$ . The optimal threshold $j^*$ which is also regarded as the number of the group into which the maximum variance of the between-class, i.e. $(\sigma_B^2)_{max}$ , falls with the corresponding group $\Omega_{j^*}$ is defined as:

$$j^* = \boldsymbol{argmax}_{\mathbf{0 \le j \le M_z - 1}}\{\sigma_B^2(\boldsymbol{j})\}$$

After finding the optimal thresholds of the input image, a decision module is used for labeling each pixel respecting the thresholds. Consequently, the proposed method can be described by a flowchart given in Figure 1.

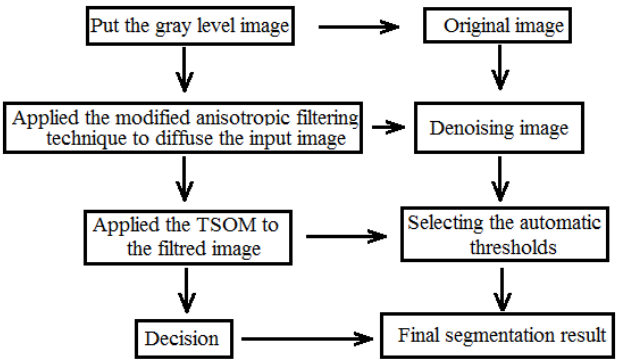


**Figure 1:** Flowchart of the proposed method.

## 3. Experimental Results

In this section, several simulation results on textured images are presented to illustrate the ideas presented in the previous section. The original images are represented on 8 bits and have an intensity range from 0 to 255. The used images database is shown in Figure 2. The patterns are numbered from 1 through 12, starting at the upper left-hand corner.

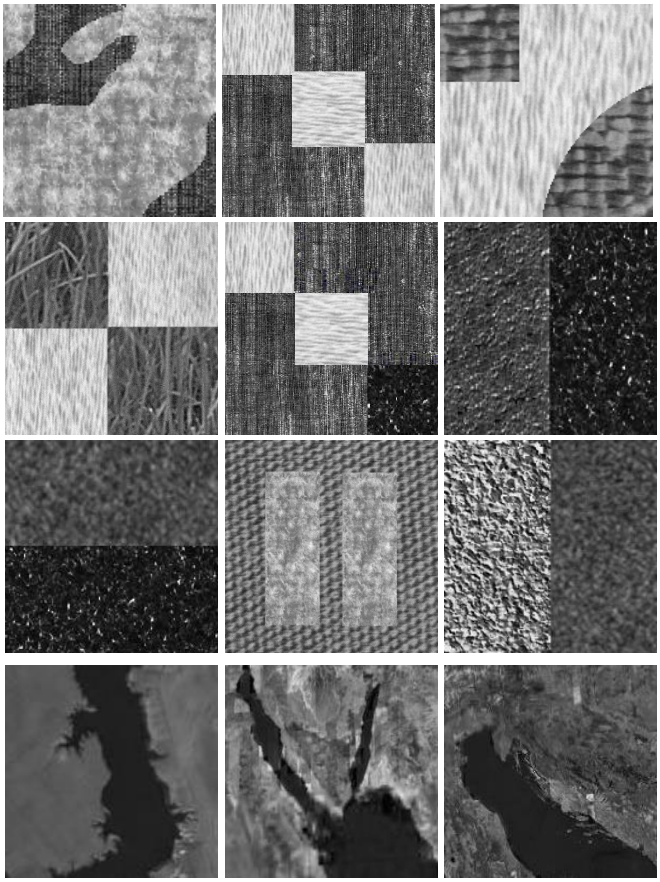

**Figure 2:** Dataset used in the experiment. Twelve were selected for a comparison study. The patterns are numbered from 1 through 12, starting at the upper left-hand corner.

Fig. 3 shows a comparison results between the different denoising models. It shows the result of applying the first step of this technique. This algorithm can be applied just to gray-scale images.

The original image shown in Fig. 3(a) is selected to show the comparison between these denoising techniques. The original image *(N × M)* is disturbed with a "salt and pepper" noise. This affects approximately *(D × (N × M))* pixels. The value of *D* is 0.02.

The final resulting images by the isotropic, anisotropic and regular anisotropic diffusion technique are shown in Fig. 3(b), 3(c) and 3(d), respectively.

Comparing the results, we can find that the result image is much better filtered in (d) that those in (b) and (c). In fact, one can find that the image was diffused within object boundary but to a much lesser amount near the boundaries of the objects. In brief, the experimental results conform to the visualized gray level distribution in the objects.

To evaluate the performance of the different denoising algorithms, its accuracy is recorded.

Regarding the accuracy, table I lists the PSNR of the different denoising methods for the data set used in the experiment.

Peak Signal-to-Noise Ratio (PSNR), Signal–to-noise ratio (SNR) is a mathematical measure of image quality based on the pixel difference between two images. The SNR measure is an estimate of quality of reconstructed image compared with original image.

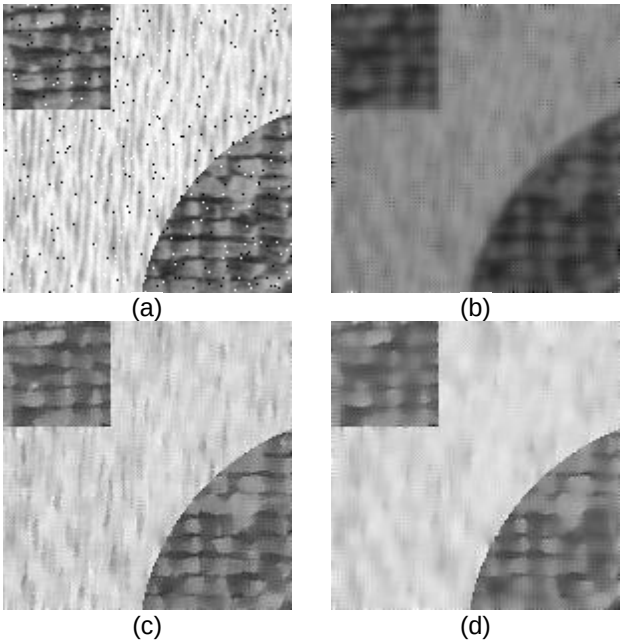


**Figure 3:** Denoising results on a gray level image, (a) Original image (256x256) with gray level spread on the range [0, 255] Disturbed with a salt and pepper noise (D=0.02). (b) Resulting image by isotropic diffusion-based method. (c) Resulting image by anisotropic diffusion-based method. (d) Resulting image by regular anisotropic diffusion-based method.

The PSNR is computed using:

$$PSNR = 10log\frac{s^2}{MSE}$$

where: s = 255 for an 8-bit image. The PSNR is basically the SNR when all pixel values are equal to the maximum possible value, and the Mean Square Error (MSE) is computed by averaging the squared intensity of the original (input) image and the resultant (output) image pixels. The MSE is calculated using:

$$MSE = \frac{1}{NM}\sum_{m=0}^{M-1}\sum_{n=0}^{N-1} e(m,n)^2$$

where e(m, n) is the error difference between the original and the distorted images

**Table1.** PSNR for 12 images show in Fig.2.

| | Isotropic diffusion method (IDM) | Anisotropic diffusion method (ADM) | regular Anisotropic diffusion method (RADM) |
|---|---|---|---|
| | PSNR | | |
| **Image 1** | 18.58 | 16.72 | 16.14 |
| **Image 2** | 13.23 | 11.91 | 10.49 |
| **Image 3** | 15.25 | 13.72 | 12.25 |
| **Image 4** | 13.73 | 12.36 | 11.93 |
| **Image 5** | 20.70 | 18.63 | 17.98 |
| **Image 6** | 15.85 | 14.27 | 13.77 |
| **Image 7** | 17.97 | 16.18 | 14.61 |
| **Image 8** | 13.73 | 12.36 | 11.93 |
| **Image 9** | 11.61 | 10.45 | 9.09 |
| **Image 10** | 22.42 | 20.18 | 19.48 |
| **Image 11** | 23.93 | 21.54 | 18.79 |
| **Image 12** | 19.79 | 17.81 | 16.19 |

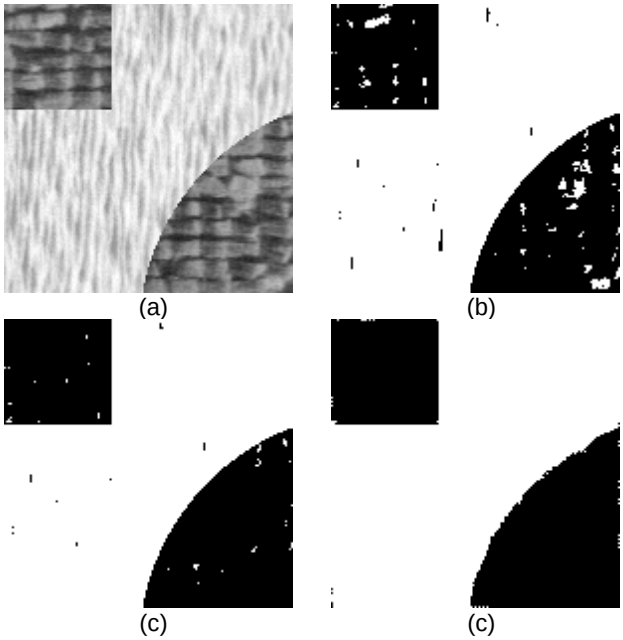


**Figure 4:** Segmentation results by TSOM algorithm combined with different filtering techniques (2 classes). (a) Original image which contains two classes, (b) segmentation based on isotropic diffusion algorithm and TSOM method, (c) segmentation based on anisotropic diffusion algorithm and TSOM method, (d) segmentation based on regular anisotropic diffusion algorithm and TSOM method (our method).

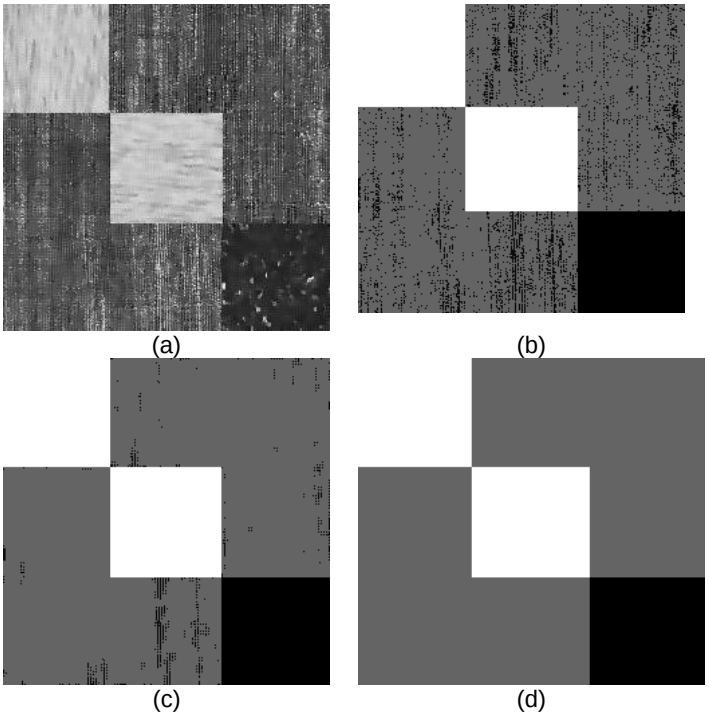


**Figure 5:** Comparison of the proposed segmentation method with other existing methods on a textured image (3 classes). (a) original image which contains three classes (b) segmentation based on anisotropic diffusion algorithm and FCM method, (d) segmentation based on anisotropic diffusion algorithm and TSOMDS method (our method), (f) reference segmented image.

It can be seen from table 1 that the performance of the regular anisotropic diffusion is quite acceptable. In fact, one can observe in Figure 4(b) and 4(c) that 15.25 and 13.72 of PSNR obtained by the isotropic and anisotropic diffusion methods, respectively. Indeed only 12.25 of PSNR were presented in Figures 4(d).

The segmentation results obtained by applying the TSOM and TSOM algorithms to the input images, which contain two and three classes, are shown in Fig. 4 and Fig. 5, respectively.

The obtained result presented in Fig (4. (c)) is a black and white image shows that the two classes are distinctly separated.

In figure 5, a label to each pixel corresponding to the class to which it belongs is affected. However, for easy viewing, the label of each class is selected by the user. It is noted that the three classes are perfectly built by using the proposed method.

In this context, one can find that the image segmentation by using anisotropic filtering combined with the multilevel thresholding technique appears to be an interesting method for gray level images.

In short, the proposed algorithm outperforms all these well-known segmentation algorithms in terms of segmentation sensitivity (Sen(%)).

Table 2 shows the obtained results for the images presented in Figure 2. We notice that the discussed proposed method allows to give very competitive results, compared with other well-known segmentation algorithms in terms of the segmentation sensitivity over the set of images of the textured and satellite images database.

To evaluate the performance of the proposed segmentation algorithm, its accuracy was recorded. Regarding the accuracy, Table 2 lists the segmentation sensitivity of the proposed method and the FCM algorithm for the data set used in the experiment.

**Table 2:** Segmentation sensitivity From RADM and FCM, RADM and TSOM for the Data set Shown in Fig. 2

| | FCM AND RADM | TSOM AND RADM |
|---|---|---|
| | Sensitivity segmentation (%) | |
| **Image 1** | 85.88 | 93.37 |
| **Image 2** | 81.45 | 91.11 |
| **Image 3** | 73.03 | 88.86 |
| **Image 4** | 88.33 | 93.19 |
| **Image 5** | 77.84 | 90.99 |
| **Image 6** | 71.61 | 84.36 |
| **Image 7** | 72.91 | 81.20 |
| **Image 8** | 60.87 | 83.24 |
| **Image 9** | 72.65 | 92.24 |
| **Image 10** | 63.78 | 88.86 |
| **Image 11** | 74.78 | 85.48 |
| **Image 12** | 76.50 | 85.20 |

The segmentation sensitivity [18] [19] is computed using:

$$Sens(\%) = \frac{N_{pcc}}{N \times M} \times 100$$

with: *Sens(%)*, $N_{pcc}$, $N \times M$ correspond respectively to the segmentation sensitivity (%), number of correctly classified pixels and image dimension.

The performance of the proposed method is quite acceptable. In fact, from table 2, one can observe in Figures 5(b) that 22.16% of pixels were incorrectly segmented for the RADM and FCM algorithm. However, only 9.01% of pixels were incorrectly segmented by the proposed method.

This experiment shows the validity of our proposed hybrid method and the significant improved performance in segmentation. In short, the proposed algorithm improve the obtained results in terms of segmentation sensitivity (Sen(%)).

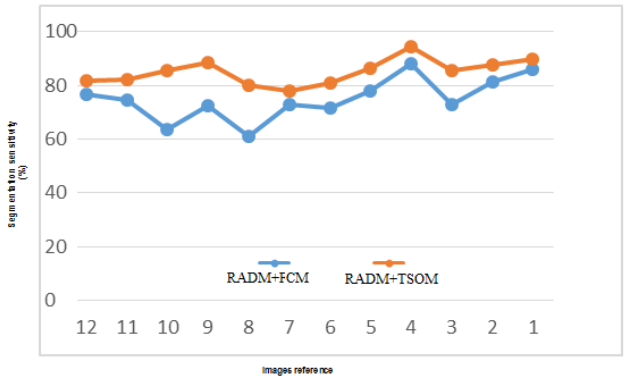


**Figure 6:** Segmentation sensitivity plots using FCM and RADM, TSOM and RADM for the Data set Shown in Fig. 2.

The segmentation sensitivity values reported in Table 2 is plotted in Figure 6.
As seen on Figures 6, the proposed method plot is clearly located on the top of the other methods plots.

## 4. Conclusion

In this paper, we have proposed a new gray level image segmentation method based on anisotropic filtering and multilevel thresholding. This method consists of two steps. In the first step, anisotropic filtering technique is used to filter the original image. In the second step, an optimal multi-level thresholding is used based on the two-stage Otsu optimization approach to segment the input image into homogeneous regions.
The obtained results demonstrated the significant improved performance in segmentation. The proposed method can be useful for gray level image segmentation.

## 5. References

[1]. M. Sezgin and B. Sankur, "Survey over image thresholding techniques and quantitative performance evaluation", Journal of Electronic Imaging, vol. 13, pp. 146-165, 2004.
[2]. G. Jing, D. Rajan and C. E. Siong, "Motion detection with adaptive background and dynamic thresholds", In: IEEE Internt. Conf. Information, Communications and Signal Processing, Bangkok, Thailand, December, pp. 41–45, 2005.
[3]. S. Ben. Chaabane, M. Sayadi, F. Fnaiech and E. Brassart, "Color Image Segmentation using Automatic Thresholding and the Fuzzy C-Means Techniques", IEEE MELECON, pp. 857-861, 2008.
[4]. Z. Hou, Q. Hu and W. L. Nowinski, "On minimum variance thresholding", Pattern Recognition Letters, vol 27, pp. 1732-1743, 2006.
[5]. O. Demirkaya and M. H. Asyali, "Determination of image bimodality thresholds for different intensity distributions", Signal Processing: Image Communication, vol. 19, pp. 507-516, 2002.
[6]. N. Otsu, " A threshold selection method from gray-level histogram", IEEE Trans. Systems Man Cybernet., no.8, pp. 62–66, 1979.
[7]. D. Y. Huang and C. H. Wang, "Optimal multi-level thresholding using a two-stage Otsu optimization approach", Pattern Recognition Letters, vol. 30, pp. 275–284, 2009.
[8]. S. Greenberg and D. Kogan, "Improved structure adaptive anisotropic filter", Pattern Recognition Letters, vol. 27, no. 1, pp. 59-65, 2006.
[9]. L. Rudin and S. Osher,"Total Variation based image restoration with free local constraints", `Proceedings of IEEE International Conference on Image Processing, vol. 1, pp. 31-35, 1994.
[10]. C. Tomasi and R. Manduchi,"Bilateral Filtering for Gray and Color Images", Proceedings of ICCV, pp. 836-846, 1998.
[11]. M. Elad, "On the origin of the bilateral filter and ways to improve it", IEEE Transactions on Image Processing, vol. 11, no. 10, 1141-1151, 2002.
[12]. A. Buades, B. Coll, and J. Morel, "Nonlocal image and movie denoising," International Journal of Computer Vision, vol. (to appear), 2007.
[13]. M. Mahmoudi and G. Sapiro, "Fast image and video denoising via nonlocal means of similar neighborhoods," IEEE Signal Processing Letters, vol. 12, no. 12, pp. 839–842, December 2005.
[14]. N. Wiener, "Extrapolation, Interpolation, and Smoothing of Stationary Time Series", New York: Wiley, 1949.
[15]. J. Portilla, V. Strela, M. Wainwright, M., and E. Simoncelli, "Image denoising using scale mixtures of Gaussians in the wavelet domain", IEEE Transactions on Image Processing, vol. 12, no. 11, pp. 1338-1351, 2003.
[16]. Q. Li and C. He, "Application of Wavelet Threshold to Image De-noising," In Proceedings of ICICIC, vol. 2, pp.693-696, 2006.
[17]. P. Perona, J. Malik, Scale space and edge detection using anisotropic diffusion, Proc. IEEE Comp. Soc. Workshop on Computer Vision (Miami Beach, Nov. 30 – Dec. 2, 1987), IEEE Computer Society Press, Washington, 16–22, 1987.
[18]. Grau V, Mewes AUJ, Alcaniz M, Kikinis R, Warfield SK: Improved watershed transform for medical image segmentation using prior information. IEEE Trans Med Imag 2004, 23(4):447-458. 10.1109/TMI.2004.824224.
[19]. Duda RO, Hart PE, Sork DG: Pattern Classification. Wiley-Interscience, New York; 2000.

## Author Profile

Slim BEN CHAABANE born in 1979 in Chebba (Tunisia), she received the BSc degree in Electrical Engineering and the DEA degree in Automatic and Signal Processing at the High school of sciences and techniques of Tunis, respectively in 2004 and 2006.

It received the PhD in Digital image processing at the High school of sciences and techniques of Tunis in collaborating with University of Picardie Jules Verne, France in 2009.
Its research interests are focused on signal Processing, image processing, classification, segmentation and data fusion.